GEOLOGICAL AND GEOCHEMICAL FEATURES OF THE KOPAONIK INTRUSIVE COMPLEX (VARDAR ZONE, SERBIA)

Mario Zelic*, Samuele Agostini°, Michele Marroni*,°,✉, Luca Pandolfi*,° and **Sonia Tonarini°**

* *Dipartimento di Scienze della Terra, Università di Pisa, Italy.*
° *Istituto di Geoscienze e Georisorse, CNR, Pisa, Italy.*
✉ *Corresponding author, e-mail: marroni@dst.unipi.it*

Keywords: *granitoids, geochemistry, Rb-Sr dating, extensional tectonics, Oligocene. Kopaonik, Serbia.*

ABSTRACT

In the Vardar Zone of the Dinaric-Hellenic Belt, several intrusive magmatic bodies with an age spanning from Early Cretaceous to Miocene occur. One of the main bodies is represented by the Kopaonik Intrusive Complex that crops out in Southern Serbia in an area of about 90 km^2. This paper deals with the geological and geochemical features of the Kopaonik Intrusive Complex, in order to provide useful constraints for its interpretation in the frame of the post-collisional magmatic activity that characterized the more internal zone of the Dinaric-Hellenic Belt.

The Kopaonik intrusive complex is characterized by a dome-like structure consisting of three concentric magmatic facies, including lithotypes ranging from qtz-diorites to granodiorites and qtz-monzonites, with a gradual and continuing transition between them. The collected data indicate that the Kopaonik granitoids are I-type, with high-K calc-alkaline affinity. The origin of the intrusive complex is partially obliterated by shallow interaction between the qtz-dioritic rocks and carbonate host rocks, affecting Ca-Sr contents and $^{87}Sr/^{86}Sr$ ratios. Nevertheless, the collected geological, petrographical and petrochemical data suggest a strong genetic relationship of the three facies. A minimum emplacement age of 31.5±0.3 Ma (Early Oligocene) is provided by Rb-Sr whole-rock biotite age.

The Kopaonik intrusives belong to a continuous Late Paleogene-Middle Miocene magmatic belt developed throughout the Balkan Peninsula from the Eastern Alps to Northwestern Turkey, and linked with subduction of the NeoTethys oceanic plate under the Eurasia. In this framework, the source of the Kopaonik magmatic rocks can be identified in a mantle wedge strongly modified by subduction-induced metasomatism.

INTRODUCTION

The Dinaric-Hellenic Belt is a collisional belt derived from the Mesozoic to Tertiary convergence between the Eurasia and Adria plates. After closure of the oceanic basin(s) located between these two plates, the Dinaric-Hellenic Belt originated by collision between the pair of continental margins (Adria and Eurasia), followed by a long lived post-collisional stage. This stage has been characterized since Late Cretaceous by westward migration of the compression front across the Adria Plate associated with extension in the internal domains of the belt. As in other Alpine collisional belts, extensional tectonics was accompanied by widespread magmatism, whose characteristics provide valuable insights for reconstructing the post-collisional stages of the Dinaric-Hellenic Belt. For instance, the ages of the different magmatic bodies, their geochemical affinity and the assessment of a chronological trend across the belt are very important for geodynamic reconstructions. Despite the importance of this magmatism, its characteristics have not been yet deeply investigated and a complete dataset is still lacking.

In this paper, a complete study of the Kopaonik intrusive complex, one of the main intrusive bodies of the Dinaric-Hellenic Belt (Vardar Zone, Serbia) is presented. This study has been performed through the integrated approach of field and laboratory analyses that allowed drawing a complete picture of this intrusive complex in the context of the Dinaric-Hellenic Belt.

THE TECTONIC FRAMEWORK OF THE DINARIC-HELLENIC BELT

The Dinaric-Hellenic Belt (Fig. 1) is an orogenic chain of Alpine age about 2000 km long, derived from the Mesozoic to Neogene convergence between the Adria and Eurasia Plates. In the classical reconstructions, the evolution of this belt includes a rifting stage developed during Early Triassic along the northern margin of Gondwanaland (e.g., Dimitrijević, 2001; Pamić et al., 2002; Bortolotti et al., 2005; Robertson et al., 2009). The rifting process, characterized by thick sedimentation of syn-rift deposits and alkaline magmatism, evolved into oceanic spreading during the Middle to Late Triassic (e.g., Bortolotti et al., 2007; 2008). The following spreading and drifting phases resulted in the development of a wide basin characterized by mid-ocean ridge (MOR) oceanic lithosphere (Pamić et al., 2002; Bortolotti et al., 2004; 2005; Saccani et al., 2004). This oceanic basin, with (Karamata et al., 2000; Dimitrijević, 2001; Karamata, 2006; Robertson et al., 2009) or without (Pamić et al., 1998; Pamić et al., 2002; Bortolotti et al., 2005) a microcontinent within it, was located between the Adria and Eurasia continental margins. Convergence began during Early Jurassic, with the development of an intraoceanic subduction followed by formation of new oceanic lithosphere in the related supra-subduction basin (e.g., Saccani et al., 2008a and 2008b). As a consequence of convergence, the obduction took place, resulting in the emplacement of oceanic lithosphere slices onto the continental margin of the Adria Plate during the Middle to Late Jurassic (Çollaku et al., 1992; Robertson and Karamata, 1994; Dimitrijević, 1997; Pamić et al., 2002; Bortolotti et al., 2004; 2005; Dilek et al., 2005; Gaggero et al., 2009). The continuous convergence between Adria and Eurasia led subsequently to continental collision, which age is still matter of debate. Some authors (e.g., Robertson and Karamata, 1994; Bortolotti et al., 2005) have proposed a Late Jurassic - Early Cretaceous age, whereas others (e.g., Pamić et al., 2002; Schmid et al., 2008) suggested that continental collision occurred during Late Cretaceous - Early Paleogene. After continental collision and up to Neogene time, continuous convergence, still active today, affected the continental margin of the Adria Plate, that was progressively deformed in westward-verging, thick-thinned thrust sheets. This geodynamic evolution produced the present-day structural pattern of the Dinaric-Hellenic Belt, represented by an assemblage of northwest-southeast to north-south trending Zones, corresponding to the modern concept of tectonic units (see discussion in Bortolotti et al., 2004). Each Zone thus consists of an assemblage of variably deformed and metamorphosed tectonic units of oceanic and/or continental origin. Along a northern transect of the Dinaric-Hellenic Belt, running from Serbia to Bosnia and Croatia, four main zones can be identified. They are, from west to east: 1- The Deformed Adria Zone, 2- the External ophiolite Belt, 3- the Drina-Ivanjica Zone and the 4 - Vardar Zone. They are bounded to the west by the undeformed Adria Zone, today located in the Adriatic Sea, and to the east by the Serbo-Macedonian-Rhodope Massif, generally regarded as part of the stable Eurasia Plate margin (Fig. 1). In this frame the Vardar Zone is regarded as a suture zone developed after collision between the Eurasia and Adria Plates compressive deformation identified in the Adria Plate (Kilias et al., 1999; Zelić et al., 2010). This extensional tectonics was characterized by high-angle normal faulting parallel to the trend of the compressional structures, and produced intramontane basins filled by continental deposits. In addition, extension was associated to widespread and long-lived magmatism, occurring throughout the Vardar Zone from Southern Greece to Northern Serbia (Cvetković et al., 2007b).

OVERVIEW OF SYN- AND POST-COLLISIONIAL MAGMATISM IN THE DINARIC-HELLENIC BELT

As previously described, the collisional and post-collisional stages are associated to extensional tectonics and a widespread magmatism, both located in the internal zones of the Dinaric-Hellenic Belt. The oldest collision-related magmatism is represented by the emplacement of Late Jurassic calk-alkaline granitoids in the Vardar Zone at the junction with the Serbo-Macedonian Massif. According to Šarić et al. (2009), the granitoids of the southern Vardar Zone can be interpreted as formed by magmatic underplating of mantle-derived magmas in the lower continental crust during the overthickening of the crust connected with collision. In the Northern Vardar Zone, the granitoids show heterogeneous features, for example the ones with low-Sr content are comparable to those from the southern areas, whereas the high-Sr ones probably formed during obduction of the ophiolites by melting of the underlying sedimentary rocks (Šarić et al., 2009). In Tertiary time, the Vardar Zone was characterized by the emplacement of I-type granitoids ranging in age from Early Eocene to Late Oligocene. The granitoids have been divided by Pamić and Balen (2001) in Eocene syn- and Oligocene post-collisional types, showing different features. The Eocene granitoids, which are mainly represented by transitional S/I-types, occur in the Prosara and Motajica Mts. In the first area (Pamić and Lanphere, 1991) they consist of alkali-feldspar granites, alkali-feldspar syenites with rare diorite, whereas in the Motajica Mt. granodiorites, monzogranites and subordinate quartz-diorites and monzodiorites are found. The S/I-type granitoids range in age from 48.7 to 55 Ma, by Rb-Sr isochron age. By contrast the Oligocene granitoids, that are found in the Boranja, Cer, Bukulja and Kopaonik Mts., are mainly of I-type (Pamić and Balen, 2001 and quoted references). These rocks span in age from 33.7 to 29.6 Ma by K-Ar datings, and range from leucogranites, tonalites and granodiorites to quartz-diorites and quartz-monzonites. Younger granitoids, ranging in age from 24 to 17 Ma (K/Ar date), have been found in the Goljia and Željin Mts. where granodiorites, quartz-monzonites, monzogranites, quartz-diorites and tonalites crop out. Like the Oligocene ones, also the Miocene granitoids are regarded by Pamić and Balen (2001) as post-collisional magmatic bodies. Thus, a continuous magmatic intrusive activity ranging in age from Late Jurassic to Miocene is testified by the rocks found along the Vardar Zone.

Also volcanic and subvolcanic rocks are widespread in the same time span. Andesites interlayered in the sedimentary deposits of Turonian and Senonian age have been described by Djordjević (2005) in the Vardar Zone of eastern Serbia. In addition, basanites, whose ages range from 40 to 60 Ma, have been reported by Cvetković et al. (2007b) along the eastern margin of the Serbo-Macedonian Massif. The basanitic rocks, regarded as emplaced at the beginning of the post-collision collapse of the Dinaric Belt, are interpreted as originated by partial melting of a supra-subduction

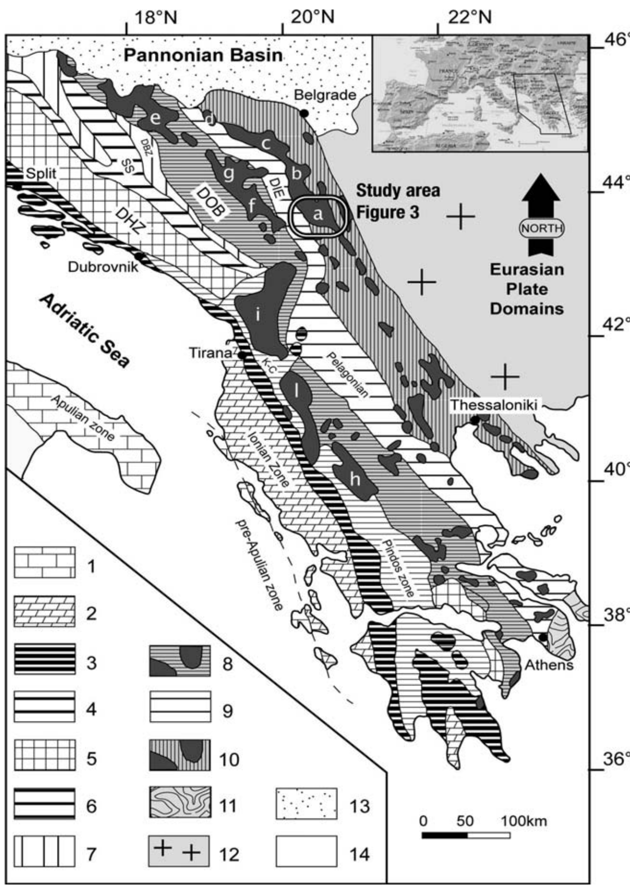

Fig. 1 - Tectonic sketch-map of the Dinaric-Hellenic Belt. Legend and abbreviations: 1- Apulian and Pre-Apulian Units; 2- Ionian Units; 3- South Adriatic Units: Kruja, Gavrovo and Tripolitsa; 4- Budva, Krasta-Cukali (K-C) and Pindos Units; 5- Dalmatian-Herzegovian (DHZ) Units; 6- Sarajevo-Sigmoid (SS) Unit; 7- East Bosnian-Durmitor Unit; 8- Dinaric Ophiolite Belt (DOB); 9- Drina-Ivanjica and Pelagonian Units (DIE); 10- Vardar Units (VZ); 11- Lavrion Blueschist Unit; 12- Serbian-Macedonian Massif; 13- Pannonian Basin; 14- Bradanic trough. Ophiolites: a- Ibar; b- Troglav; c- Maljen; d- Zvornik; e- Krivaja-Konjuh; f- Bistrica; g- Zlatibor; h- Pindos; i- Mirdita; j- Chalkidiki; k- Goles. The location of Fig. 3 (study area) is indicated.

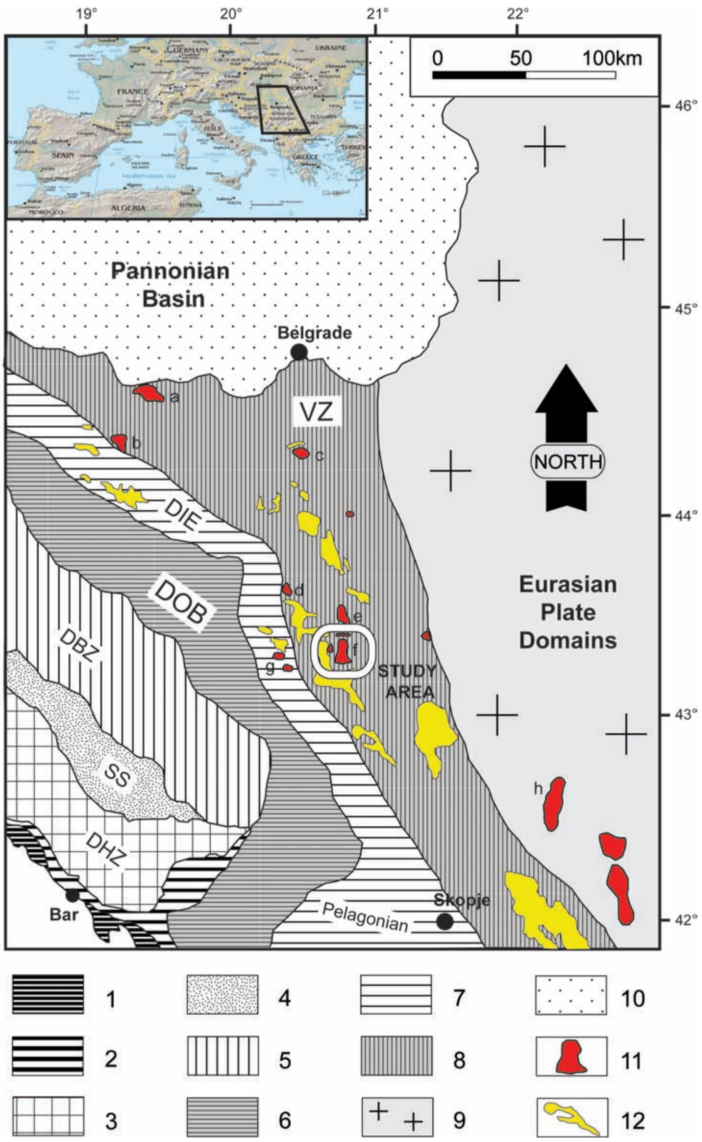

Fig. 2 - Tectonic sketch of a segment of the Dinaric-Hellenic Belt and simplified map of Tertiary magmatic formations in Serbia (modified after Dimitrijević, 1997 and Karamata et al., 1992). Legend and abbreviations: 1- South Adriatic zone: Kruja, Gavrovo and Tripolitsa; 2- Budva zone, Krasta-Cukali (K-C) and Pindos; 3- Dalmatian-Herzegovian (DHZ) zone; 4- Sarajevo-Sigmoid (SS) zone; 5- East Bosnian-Durmitor zone; 6- Dinaric Ophiolite Belt (DOB); 7- Drina-Ivanjica and Pelagonian zones (DIE); 8- Vardar zone (VZ); 9- Eurasian Plate Domains; 10- Pannonian basin; 11- Magmatic intrusions 12- Volcanic rocks.
Main Tertiary magmatic intrusions in Serbia and theirs age (Ma): a- Cer intrusion (33-22); b- Boranja intrusion (33.7-29.6); c- Bukulja intrusion (27); d- Polumir-Čemerno intrusion (19-14); e- Željin intrusion (24-17); f- Kopaonik intrusion (31.2-31.8); g- Golija intrusion (20-17.5); h- Surdulica intrusion (32-42), age from Pamić and Balen (2001 and reference therein). The location of Fig. 3 (study area) is indicated.

mantle during roll-back and/or break-off of a subducting slab (Cvetković et al., 2007a). In the same geodynamic setting may have formed the Late Eocene to Oligocene shoshonite and high K calc-alkaline associations, that are very common as large exposures in the Zletovo-Kratovo, Lece Radan and Srebenica-Maglaj areas, Northern Serbia. Volcanic bodies are also recognized underground in the Pannonian Basin by deep oil-wells. Their ages range from 36 to 25 Ma (K/Ar data, Karamata et al., 1992b; Karamata, 1994; Pamić, 1997; Pamić et al., 2000; Cvetković et al., 1995). Also Miocene calc-alkaline rocks, including basalts, andesitic basalts, andesites, dacites and trachyandesites, are found in northern Serbia. Their ages range from 19.7 to 25.9 Ma (K/Ar data, Pamić, 1997; Cvetković et al., 2000). The youngest volcanic activity, ranging in age from 16.8 to 8.6 Ma (Middle to Late Miocene), is represented by basalts, andesitic basalts, dacites and rhyolites found in Northern Serbia. This magmatism is related to the extensional phases connected with the Pannonian Basin formation.

On the whole, the Late Jurassic to Miocene magmatism of the Vardar Zone resulted from a complex geodynamic history that spanned the collisional and post-collisional stages in a supra-subduction zone. The Paleocene to Miocene post-collisional stage was characterized by extensional tectonics in the supra-subduction lithosphere.

THE KOPAONIK INTRUSIVE COMPLEX

Field evidence

According to Dimitrijević (1997), the Kopaonik Intrusive Complex occurs in the geological map as a N-S elongated body with dimensions of about 15 x 6 km. Its outcrop area covers about 90 km^2, with an appendix of 5 km^2 located near Kremići, west of the main body. The intrusive complex can be described as an elongated dome with onion-like structure consisting of three concentric magmatic facies, hereafter referred to as A, B and C (Fig. 3). According to Urošević et al. (1973a) the transition between these magmatic facies is gradual and continuous, without clear sharp contacts between them. The core of the Kopaonik Intrusive Complex is represented by porphyroid qtz-monzonites and minor granodiorites (facies C), characterized by coarse-grained texture with cm-long crystals, up to 3 x 5 cm, of K-feldspar and amphibole. In the map, the orientations of the long axes of these minerals are roughly distributed in a dome-like shape with a continuous strike change from a N-S trend in the western and eastern areas to an E-W trend in the northern and southern areas. The apparent thickness of facies C is about 3 km, but its true thickness is very difficult to assess, owing to the gradual transition with the neighbouring facies B. In turn, facies B consists of granodiorites and qtz-monzodiorites, medium grained to the north and fine grained to the south. Its apparent thickness ranges from 1 km, in the southern area, to 2-3 km in the northern one. In turn, facies A consists of fine-grained qtz-diorites, with a well developed magmatic foliation consisting of well-oriented crystals of plagioclase, K-feldspar, biotite and amphibole. The foliation shows the same trend detected in facies C, with a continuous change from N-S in western and eastern areas to E-W in the northern and southern areas. The thickness of facies A exceeds 2-3 km. The minor body of Kremići consists of fine-grained qtz-diorites analogous to those recognized in facies A.

In addition, along the northwestern margin of the Kopaonik Intrusive Complex, stocks and dykes of rocks with dioritic and qtz-dioritic composition cutting the granodiorites and qtz-monzodiorites of facies B have been detected (Dimitrijević, 1997). Different types of enclaves with variable dimensions and shape, from rounded to sub-rounded, occur. They are microgranular to porphyritic with abundant amphibole and biotite. The enclaves are roughly parallel to the foliation trend detected in facies C and to the preferred orientation of phenocrysts in facies A (Cvetković et al., 2002).

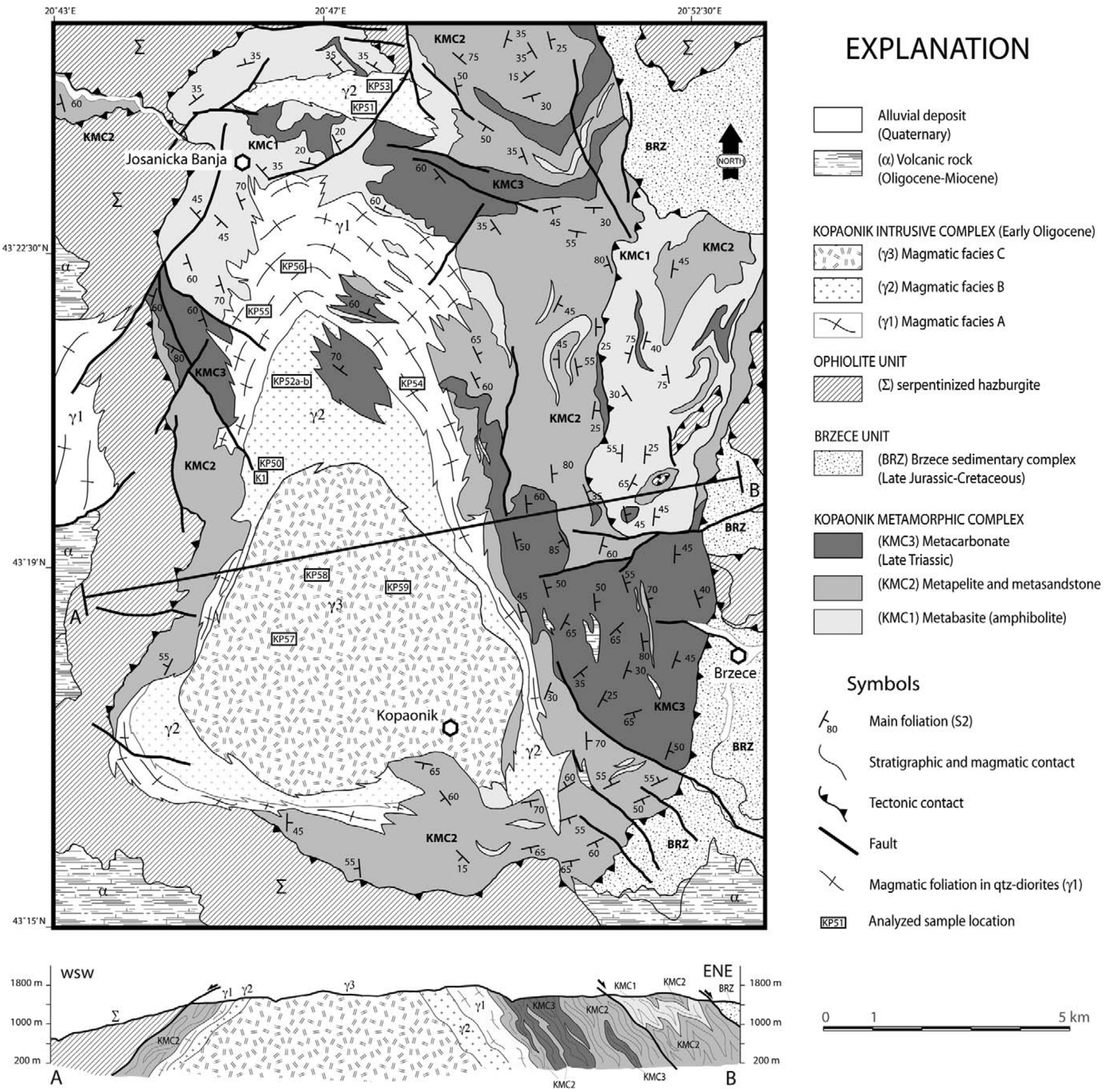

Fig. 3 - Simplified geological sketch-map of the Kopaonik area and related cross-section. The locations of the studied samples are also indicated.

According to the map distribution of the tree facies, the qtz-monzonites of facies C lie at the core (lowermost level) and the qtz-diorite of facies A (uppermost level) is at the contact with the host rocks (Fig. 3), which belong to the Kopaonik Metamorphic Complex (Zelić et al., 2010). This latter consists of a thick meta-carbonate succession associated to minor meta-pelites and amphibolites. Whereas the meta-carbonates and meta-pelites are attributed to the Late Triassic (Sudar, 1986), the age of the amphibolites is still unknown. According to Zelić et al. (2005), the amphibolites can be regarded as post-Variscan magmatic rocks, but their geodynamic significance is still matter of debate. In turn, the Kopaonik metamorphic complex is topped, from bottom to top, by the Brzece Unit, the Ophiolite Unit and the Brus Unit (Marroni et al., 2004; Zelić et al., 2010). The contact between host rocks and intrusive body is marked by a thermo-metamorphic aureole (Urošević et al., 1973a), which is best exposed along the eastern and southern margin of the Kopaonik Intrusive Complex. This aureole is represented by scarns and hornfels, with a thickness up to 1500 m along the margin of the intrusion. The skarns are characterized by the occurrence of andalusite, wollastonite and/or garnet, with the latter mineral up to 2-3 cm in size. The hornfels, mainly exposed along the eastern and southern margin of the Kopaonik Intrusive Complex, are composed by an andesine, diopside, actinolite and quartz mineral assemblage. It is noteworthy that no sediments lying unconformably on the intrusive complex and/or on the host rocks have been identified, however, in the western area scattered outcrops of dacites and andesites of probably Miocene age occur at the top of the Kopaonik Metamorphic Complex.

Petrography and major-element chemistry

The mineral paragenesis for all three facies of the Kopaonik Intrusive Complex is plagioclase, quartz, orthoclase, amphibole, biotite, plus scarce (≤ 1% by volume) magnetite and accessory minerals (e.g., zircon, apatite). However, the mineral proportions are very different in each facies (Table 1, Fig. 4): in facies A plagioclase is largely the most abundant phase (55-60% in volume), and amphibole (≈ 20%) is dominant over biotite (10-17%), quartz (6%) and

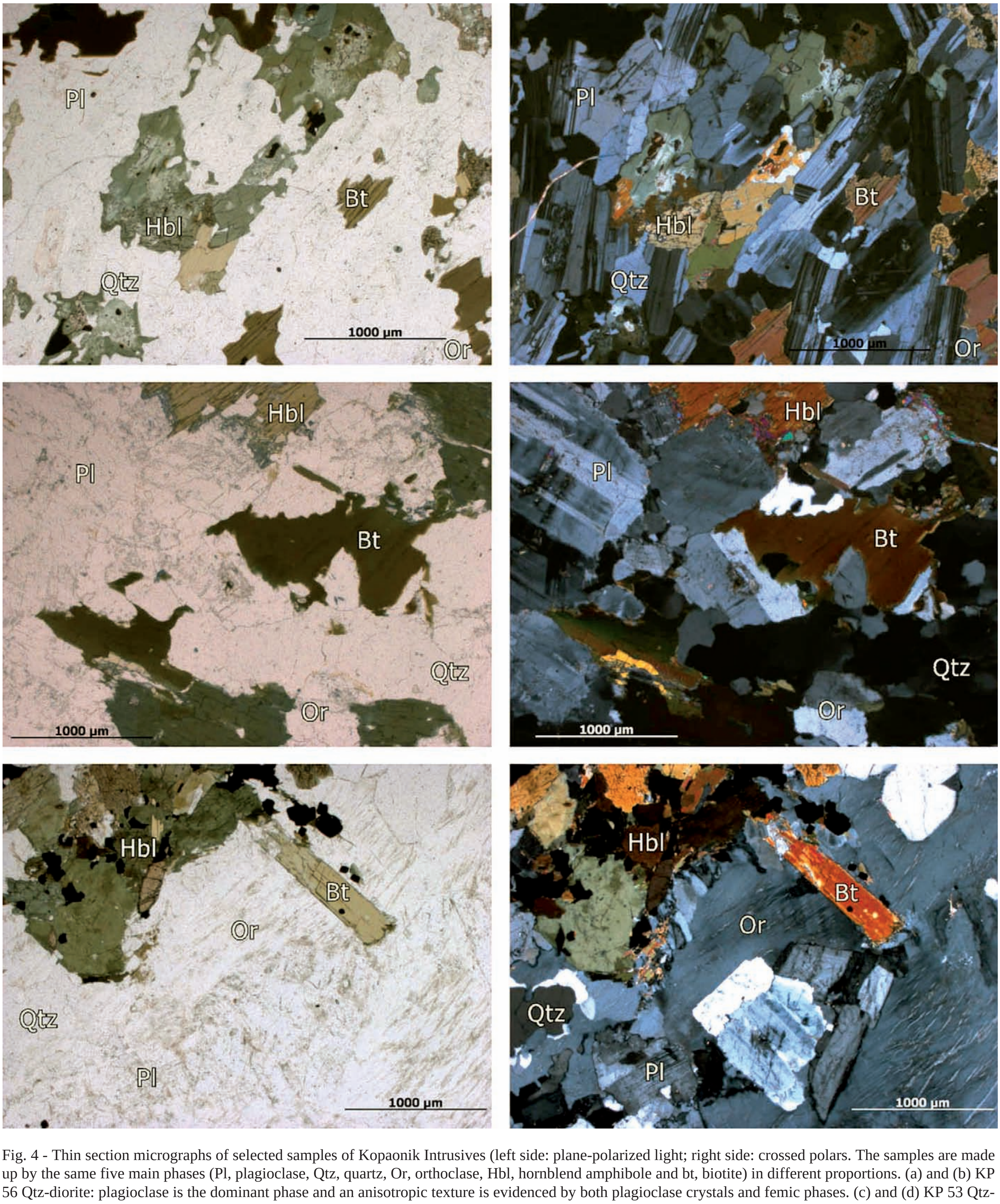

Fig. 4 - Thin section micrographs of selected samples of Kopaonik Intrusives (left side: plane-polarized light; right side: crossed polars. The samples are made up by the same five main phases (Pl, plagioclase, Qtz, quartz, Or, orthoclase, Hbl, hornblend amphibole and bt, biotite) in different proportions. (a) and (b) KP 56 Qtz-diorite: plagioclase is the dominant phase and an anisotropic texture is evidenced by both plagioclase crystals and femic phases. (c) and (d) KP 53 Qtz-monzodiorite: here plagioclase, quartz and orthoclase have more similar abundances and the texture is more equigranular and isotropic with respect to KP 56. (e) and (f) KP 57 Qtz-monzonite: this sample is characterized by big perthitic orthoclase crystals, smaller quartz and plagioclase and quite rare femic minerals, which are often found in aggregates.

Table 1 - Modal composition, major elements, trace elements and Sr-Nd isotope rations of Kopaonik intrusive rocks.

Sample	KP 55	KP 54	KP 56	KP 51	KP 53	KP 50	K 1	KP 52a	KP 52b	KP 59	KP 58	KP 57
Facies	A	A	A	B	B	B	B	B	B	C	C	C
Modal composition (vol %)												
Plagioclase		60.0	54.5		44.5				44.5	33.5		26.5
Ortochlase		1.5	2.0		8.5				10.5	38.0		48.5
Quartz		6.0	6.0		20.0				21.5	21.0		15.5
Amphibole		20.5	19.5		14.0				13.0	5.5		7.5
Biotite		10.5	17.0		12.5				10.0	2.0		2.0
Oxides		1.5	1.0		0.5				0.5	<0.5		<0.5
Major elements (wt %)												
SiO_2	53.01	53.27	54.57	57.92	59.73	60.01	60.77	60.82	61.25	64.04	64.67	64.77
TiO_2	0.86	0.88	0.88	0.77	0.76	0.70	0.72	0.65	0.66	0.55	0.47	0.47
Al_2O_3	18.40	18.55	19.15	17.37	16.79	16.99	16.92	17.12	16.78	15.69	15.96	16.10
Fe_2O_3 tot	8.08	8.05	8.11	6.77	6.07	5.97	5.85	5.54	5.74	4.32	3.99	3.93
MnO	0.14	0.15	0.14	0.14	0.12	0.12	0.11	0.11	0.11	0.09	0.08	0.08
MgO	4.61	4.64	4.68	3.19	2.84	2.70	2.75	2.54	2.66	1.51	1.41	1.35
CaO	7.88	7.86	8.09	6.26	5.52	5.74	5.51	5.30	5.37	4.06	3.89	3.76
Na_2O	3.31	3.50	3.35	3.39	3.19	3.20	3.24	3.35	3.21	3.57	3.60	3.44
K_2O	1.50	1.59	1.53	2.38	2.68	2.68	2.58	2.53	2.65	3.94	4.13	4.40
P_2O_5	0.17	0.18	0.18	0.17	0.16	0.16	0.15	0.16	0.15	0.19	0.16	0.17
L.O.I.	0.73	0.77	0.66	0.40	0.57	0.46	0.70	0.57	0.80	0.91	0.56	0.46
Total	98.69	99.44	101.34	98.76	98.43	98.73	99.30	98.69	99.38	98.87	98.92	98.93
Trace Elements (μg/g)												
Be		1.78	1.55	2.10	2.03		2.24		2.15	4.68		4.30
Sc		22	22	19	15		14		13	7		6
V		178	179	134	120		114		104	71		63
Cr		37	38	16	13		13		12	9		9
Co		22	23	16	15		14		13	8		7
Ni		16	15	8	7		7		6	4		4
Cu		14	29	15	12		7		5	3		3
Ga		19.1	19.0	18.5	17.9		18.3		17.4	17.7		17.4
Rb (ICP-MS)		74	66	95	113		115		107	195		205
Rb (xrf)		*73*	*66*	*93*	*113*		*112*		*107*	*188*		*195*
Sr (ICP-MS)		537	599	453	421		422		399	587		645
Sr (xrf)		*556*	*619*	*461*	*428*		*429*		*412*	*605*		*653*
Y		25.4	20.1	31.2	22.7		22.0		21.2	26.6		23.6
Y (xrf)		*27*	*20*	*33*	*23*		*24*		*21*	*26*		*21*
Zr (ICP-MS)		*18.7*	*19.1*	*17.7*	*10.8*		*10.1*		*14.7*	*18.6*		*18.7*
Zr (xrf)		123	133	170	163		180		188	218		187
Nb		6.6	5.1	8.1	7.8		8.4		8.3	11.7		10.3
Cs		5.0	3.5	5.8	8.9		5.5		5.4	7.3		5.9
Ba		494	523	588	637		714		706	555		851
La		19.6	20.2	29.4	25.3		24.9		29.4	47.8		47.8
Ce		41	39	58	49		48		53	90		83
Pr		5.1	4.6	6.8	5.6		5.5		5.9	10.2		9.0
Nd		20.5	17.6	26.2	20.8		20.3		20.8	36.9		32.6
Sm		4.5	3.8	5.6	4.1		4.1		4.0	7.0		6.3
Eu		1.33	1.17	1.21	1.05		1.05		0.98	1.59		1.39
Gd		4.2	3.6	5.1	3.9		3.7		3.6	5.5		4.9
Tb		0.70	0.59	0.87	0.62		0.60		0.59	0.83		0.74
Dy		4.2	3.3	5.2	3.7		3.5		3.5	4.5		3.9
Ho		0.87	0.71	1.05	0.77		0.75		0.71	0.87		0.78
Er		2.44	1.95	3.01	2.17		2.03		2.08	2.40		2.13
Tm		0.36	0.29	0.45	0.33		0.31		0.31	0.35		0.32
Yb		2.29	1.81	2.77	2.11		1.92		1.88	2.28		1.89
Lu		0.34	0.27	0.41	0.30		0.29		0.29	0.33		0.28
Hf		*0.91*	*0.89*	*0.93*	*0.60*		*0.62*		*0.74*	*0.99*		*0.85*
Ta		0.56	0.43	0.59	0.81		0.74		0.74	0.98		0.85
Tl		0.53	0.45	0.68	0.81		0.71		0.61	1.51		1.53
Pb		19.6	24.3	25.0	22.7		19.9		18.8	23.8		28.7
Th		8.1	7.8	11.0	15.8		18.6		15.1	31.3		30.6
U		1.8	1.9	2.3	4.0		5.0		3.6	8.4		8.9
Isotope Ratios												
$^{87}Sr/^{86}Sr_m$		0.706759	0.706765	0.706685	0.706871		0.706839		0.706819	0.707868		0.707847
$\pm 2\sigma_{mean}$		0.000007	0.000016	0.000009	0.000010		0.000010		0.000009	0.000008		0.000008
$^{87}Sr/^{86}Sr_i$		0.70658	0.70662	0.70641	0.70652		0.70649		0.70647	0.70744		0.70744
$^{143}Nd/^{144}Nd_m$		0.512625	0.512622	0.512581	0.512561		0.512557		0.512578	0.512492		0.512492
$\pm 2\sigma_{mean}$		0.000010	0.000006	0.000011	0.000010		0.000010		0.000013	0.000009		0.000011
$^{143}Nd/^{144}Nd_i$		0.51260	0.51259	0.51255	0.51254		0.51253		0.51255	0.51247		0.51247

Trace element data, where not specified, are ICP-MS. See Appendix for comments.
Initial Sr and Nd isotope ratios are calculated for T_0=31.5 Ma.

orthoclase (1.5-2.0%). Also in facies B, plagioclase is the most abundant phase (≈ 45%), followed by quartz (20-22%) and alkali feldspar (8.5-10%). Femic minerals are made up by amphibole and biotite. These two minerals have almost the same modal content (13-14% and 10-13%, respectively), resulting from bigger and more rare biotite crystals with respect to hornblende.

Modal abundances and petrographic texture allow facies

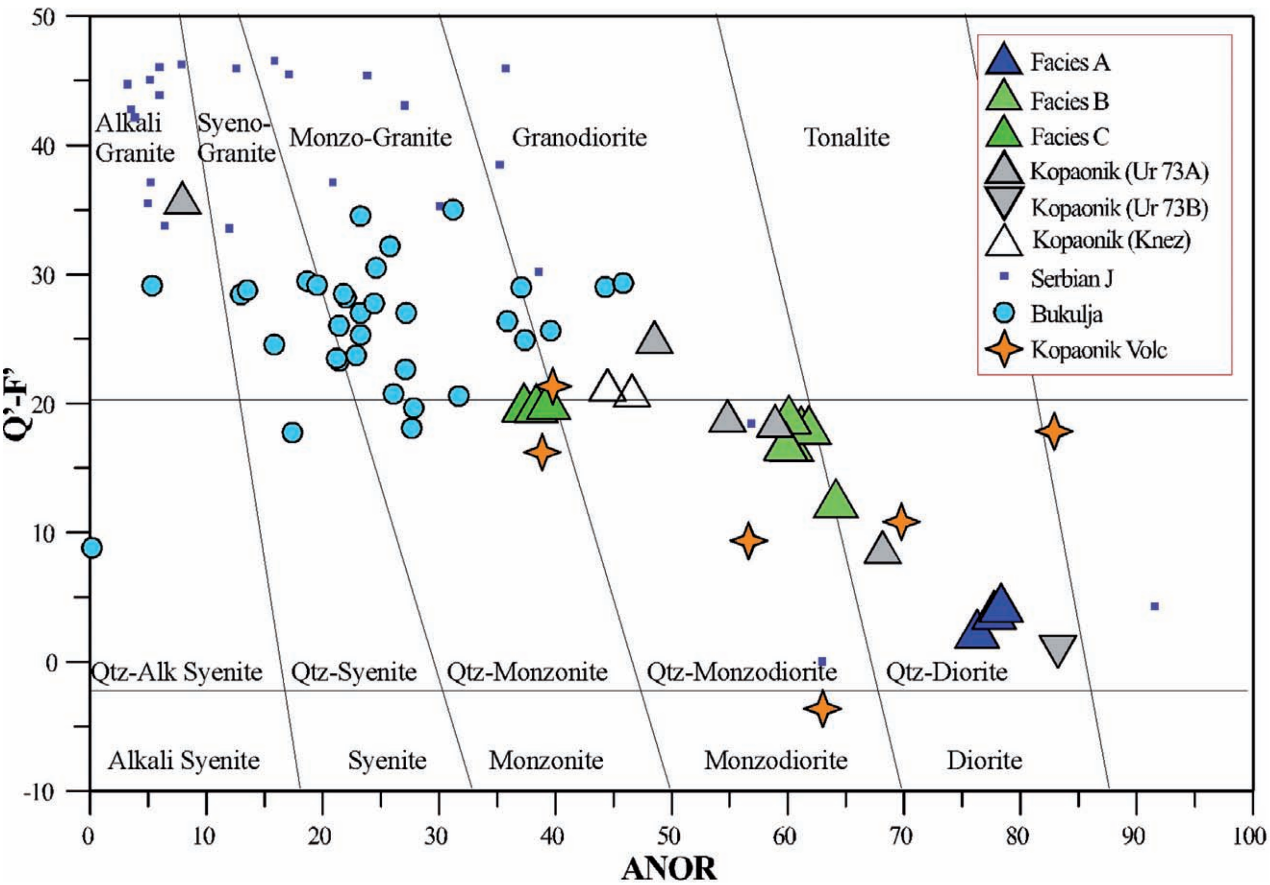

Fig. 5 - Q'-F' vs. ANOR classification diagram for plutonic rocks. Literature data for Kopaonik intrusives: Ur 73A, Urošević et al. (1973a); Ur 73B, Urošević et al. (1973b); Knežević et al. (1994). Serbian Jurassic granitoids (Serbian J) after Šarić et al. (2009); Bukulja granites after Cvetković et al. (2007b); Kopaonik volcanic rocks after Urošević et al. (1973a).

discrimination: indeed, facies A can be distinguished from facies B by an evident magmatic foliation resulting in anisotropic texture, mainly due to the orientation of plagioclase crystals, whereas facies B has equigranular isotropic texture. Lastly, facies C has a porphyritic texture, with very big and abundant orthoclase crystals (up to 2-3 cm, 38-48% by volume), subordinate plagioclase (26-33%), quartz (16-21%), and scarce amounts of amphibole (6-8%) and biotite (≈ 3%). According to the modal abundances of sialic phases, samples of facies A fall in the Qtz-diorite field of the Streckeisen double-triangle, the B facies rocks are granodiorites, whereas the C facies rocks fall close to the border between monzogranites and Qtz-monzonites.

In the Q' vs. ANOR classification diagram (Fig. 5) the rocks of A, B and C facies fall in the field of diorite, Qtz-monzodiorite and Qtz-monzonite, respectively. All the analyzed samples are metaluminous and exhibit a sub-alkaline character, as shown by the molar Al/(Na+K) ratio vs. ASI (Alumina Saturation Index, Al/(Ca+Na+K) molar ratio) of Fig. 6. The calc-alkaline affinity of the Kopaonik Complex can be stated by the K_2O vs. SiO_2 diagram (Peccerillo and Taylor, 1976), where the analyzed samples define a high-K calc-alkaline association (Fig. 7). It is noteworthy that the dioritic samples lie on the boundary between the calc-alcaline and high-K calc-alcaline series, whereas the most evolved rocks are shifted towards the shoshonitic series field.

In all the Harker diagrams the samples from the three magmatic facies are distinct and, together with the literature data (Urošević et al., 1973a; Knežević et al., 1994) they show a continuous evolution trend ranging from diorite to granodiorite fields. Most major element oxides vs. SiO_2 diagrams exhibit roughly linear negative (e.g., TiO_2, Al_2O_3, Fe_2O_3T, MgO, MnO, CaO,) or positive (K_2O) trends, whereas Na_2O and P_2O_5 are practically constant (Fig. 7, Table 1). Such trends reflect the varying proportions between the mineral phases in the different facies, in agreement with petrographic observations: for example the decrease of MgO (Fig. 7, inset), Fe_2O_3*and CaO from facies A to facies C matches the progressive decrease of modal amphibole, the Al_2O_3 variation is correlated to the plagioclase (Fig. 7, inset), whereas the increase in K_2O associated with almost constant Na_2O is associated with a switch in proportion between plagioclase and alkali feldspar.

Compatible elements are generally low (e.g., Ni ≤ 16 ppm, Cr ≤ 40 ppm), even for the diorite samples, pointing to previous extensive removal of mafic phases. In the Harker diagrams, compatible elements decrease with increasing silica content, both linearly (V, Fig. 5, Sc, Co, not shown) or not (Cr, Ni). On the contrary, incompatible elements increase with increasing SiO_2, with the exception of Sr, which exhibits upward convex trend, as does Eu (not shown). Zr contents of two samples from Knežević et al. (1994) are anomalously low, like high contents of Sr and La of another sample.

In the multi-element pattern for incompatible elements, the calc-alkaline character of the Kopaonik intrusives is confirmed by strong enrichments of Rb, Th, U, K and Pb and negative anomalies of Ta, Nb, P and Ti, with respect to

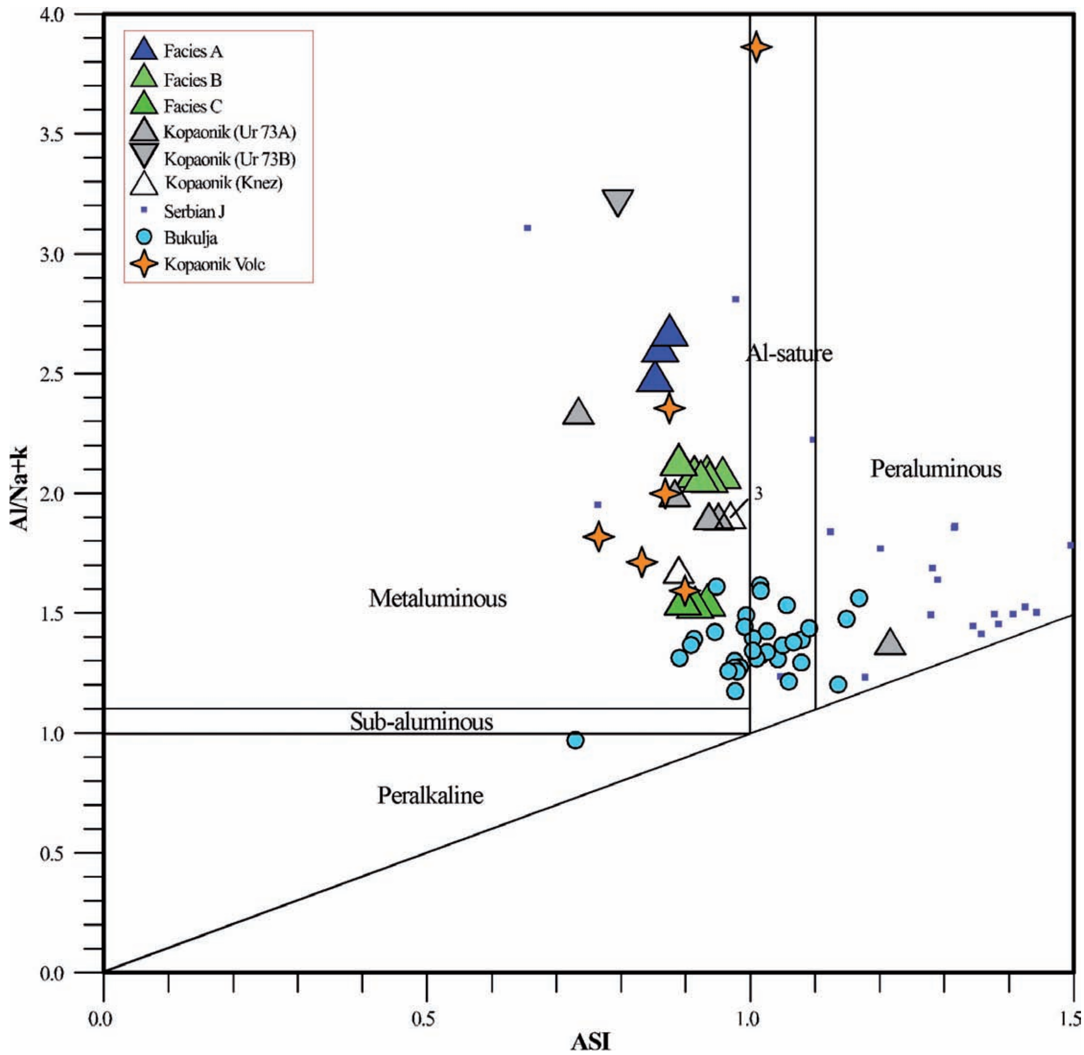

Fig. 6 - ASI (Alumina Saturation Index, molar $Al_2O_3/(CaO+Na_2O+K_2O)$ ratio) vs. Agpaitic index (molar $Al_2O_3/(Na_2O+K_2O)$ ratio). Symbols as in Fig. 4.

the Primitive Mantle (Fig. 8). Notably, the apparent negative Ba, La and Ce spikes are a mere consequence of strong alkalis and Th-U-Pb enrichment. Indeed, these latter have also strong positive anomalies with respect to the Continental Crust of Taylor and McLennan (1985).

REE patterns show higher fractionation of Light REE with respect to the Heavy REE, being the quartz monzonitic rocks the most fractionated ones (e.g., La_N/Sm_N = 4.3-4.7 and Gd_N/Yb_N = 1.9-2.1). The dioritic and qtz-monzodioritic samples exhibit minor LREE fractionation (with La_N/Sm_N = 2.8-3.3 and La_N/Sm_N = 3.3-4.6, respectively) and very low HREE fractionation (Gd_N/Yb_N = 1.5-1.7 for both). Diorites show small Eu negative anomalies (Eu_N/Eu^* = 0.93-0.95), while Eu negative anomalies are evident both in qtz-monzodiorites (Eu_N/Eu^* = 0.68-0.82) and qtz-monzonites (Eu_N/Eu^* = 0.74-0.76), indicating that evolution leading to these two facies probably involved plagioclase removal (Fig. 9).

Sr-Nd isotopes

The Kopaonik intrusive rocks show different initial Sr and Nd isotope ratios in the three facies, whereas intra-facies variations are negligible, probably also because of the limited available data-set (Table 1). As a whole, the $^{87}Sr/^{86}Sr$ initial ratio ranges from 0.7064-0.7066 for facies A and B, whereas is significantly higher for facies C (≈ 0.7074). Nd isotope values depict discrete variations, with $^{143}Nd/^{144}Nd_i$ ≈ 0.51260, 0.51254 and 0.51247 for A, B and C facies, respectively. Sr-Nd isotope ratios of the Kopaonik intrusive rocks are plotted in Fig. 10, along with other Oligo-Miocene magmatic rocks cropping out in the region. The Kopaonik intrusive rocks have Sr-Nd isotope ratios very similar to those of the high-K calc-alkaline lavas of Central Serbia, Fruška Gora-Rogozna and South Pannonia (Cvetković et al., 2004b; Pamić and Balen, 2001); moreover, they overlap the upper left end of the field depicted by the coeval ultra-K Serbian rocks (Cvetković et al., 2004b). On the other hand the Bukulja and the Cer-Boranja intrusive rocks are characterized by wider variations, which tend toward markedly higher $^{87}Sr/^{86}Sr_i$ and lower $^{143}Nd/^{144}Nd_i$ (Cvetković et al., 2007b; Pamić and Balen, 2001).

Rb-Sr isotopic age

As for many granitoids, Sr isotope heterogeneity precluded the use of the whole-rock isochron method to obtain a reliable emplacement age for the Kopanik intrusives (see below). A minimum emplacement age is provided by Rb-Sr whole-rock-biotite age, even if an element of uncertainty in the Rb-Sr age calculation results from the biotite initial Sr isotope composition that is assumed to be the same of the whole rock. However, the age results cannot be severely affected by the uncertainty of the initial Sr isotope composition determined from other minerals of the same rocks, since biotite has a high radiogenic ^{87}Sr content. In Table 2 the ^{87}Rb/^{86}Sr and ^{87}Sr/^{86}Sr determined on plagioclase, amphibole, biotite and whole rock are reported. The whole rock-biotite regression line (calculated according to the Isoplot-3 code, Ludwig, 2003) is proportional to an age of 31.4±0.3 Ma (with an initial ^{87}Sr/^{86}Sr of 0.70648 ± 0.00001); using a 4 points regression line (plagioclase, whole rock, amphibole and biotite) almost the same age (31.5 ± 0.7 Ma) and the same initial ^{87}Sr/^{86}Sr (0.70646 ± 0.00015) are obtained. These data suggest that the initial Sr isotopic disequilibrium between the mineral phases significantly increases the uncertainty on both the age and the initial isotope composition, but not the biotite isotopic age. K-Ar age determinations on five samples from Kopaonik and surroundings plutons cluster around 30-32 Ma (Karamata et al., 1992a).

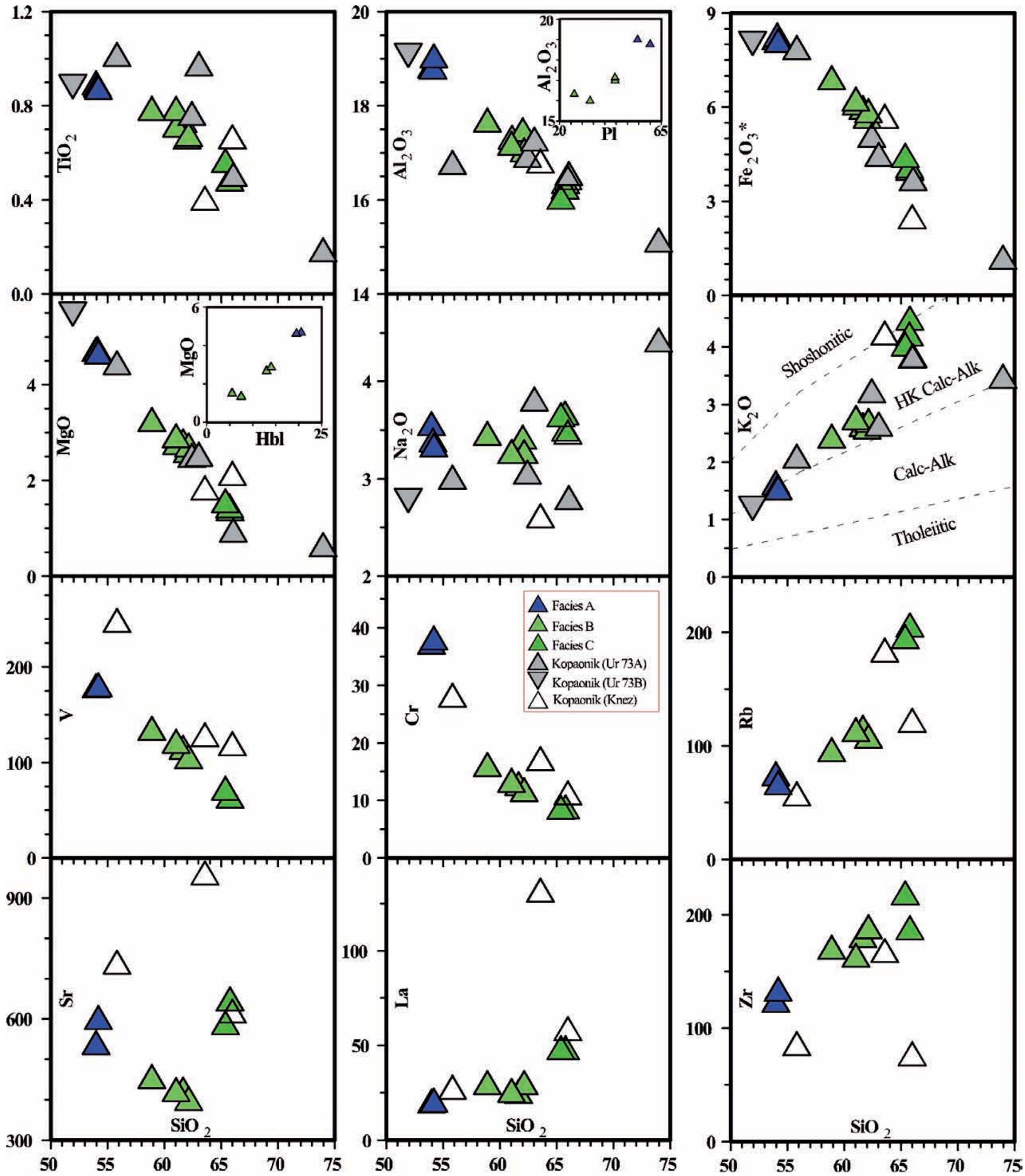

Fig. 7 - Harker diagrams for selected major and trace elements vs. SiO_2 of Kopaonik magmatic rocks. Major elements, wt%; Trace element, ppm. Symbols as in Fig. 4. Fields in K_2O vs. SiO_2 diagram after Peccerillo and Taylor, 1976). Inset of MgO vs. SiO_2 and Al_2O_3 vs. SiO_2 diagrams are MgO vs. hornblende (Hbl) and Al_2O_3 vs. plagioclase (Pl) modal abundances, respectively.

Table 2 - Rb-Sr contents and Sr isotope composition of whole rock and minerals of K1 sample.

	Rb (μg/g)*	Sr (μg/g)*	$^{87}Rb/^{86}Sr$	±2σ	$^{87}Sr/^{86}Sr$	$\pm2\sigma_{mean}$
Whole Rock	118	427	0.799	0.008	0.706839	0.000010
Plagioclase	29.4	324	0.260	0.003	0.706617	0.000010
Amphibole	40.0	44.6	2.60	0.03	0.707550	0.000040
Biotite	746	4.26	507	5.1	0.932880	0.000029

* Total Rb and Sr content were calculated considering the mean natural Rb isotope abundances and the measured Sr isotope compositions. ^{87}Rb and ^{86}Sr determined by isotope dilution method via Thermal Ionization Mass Spectrometry.

DISCUSSION

Geochemical and isotope data indicate that the Kopaonik granitoids are I-type, with high-K calc-alkaline affinity and are genetically and chemically linked to the coeval volcanic rocks analyzed by Urošević et al. (1973a). The plutonic complex may be distinguished into three facies, according to its petrochemical characters. However, the geology (gentle transition among the facies), as well as the petrography (same paragenesis with shifts among minerals relative abundances) and geochemistry (major and trace element variations without evident compositional gaps) indicate a strong genetic relationship between the different facies. Cvetković et al. (2002) reported the occurrence of enclaves into the Kopaonik granitoids; these enclaves may have similar compositions to the Kopaonik host rocks, or they may be mafic hbl-bt rich enclaves formed by cumulus processes. Their occurrence strengthens the hypothesis of a genetic link among the three facies.

The most simple relation could be through crystal fractionation in a closed system, as cumulitic enclaves are indicative of crystal fractionation processes. Nevertheless, this simple model of fractionation in a closed system does not fit with the observed Sr-Nd isotope ratios. The geochemical-isotope variations of the studied rocks may thus be attributed to mixing between a mafic magma and a more evolved one (plus some extent of fractional crystallization), or to fractional crystallization combined with assimilation of crustal material. We modeled (i) mixing between the least and the most evolved rocks of our dataset and (ii) an AFC process (Assimilation + Fractional Crystallization, De Paolo, 1981) as possible mechanisms to explain the observed trace element as well as Sr and Nd isotope variations. The mixing model was calculated using KP 54 and KP 57 compositions as end-members. For the AFC models, no data were found in literature for the chemical composition of the basement rocks, nor for the depth at which differentiation + assimilation processes may have occurred, thus, we chose as contaminants two metamorphic basement rocks of the Bukulja region (Cvetković et al., 2004b), and variable assimilation to fractionation ratios. More reliable constraints exist on the fractionation assemblage, which was taken according to the modal composition of less evolved samples. In Fig. 11 the modeled mixing and AFC trajectories are reported for Nd and Sr isotope ratios vs. selected trace elements: $^{143}Nd/^{144}Nd_i$ was plotted against Nd (an incompatible rare earth element), Zr (an incompatible high field strength element), V (a compatible element) and Sr (a large ion lithophile element), whereas $^{87}Sr/^{86}Sr_i$ was plotted against Sr and La. It is evident that AFC is a viable mechanism to ex-

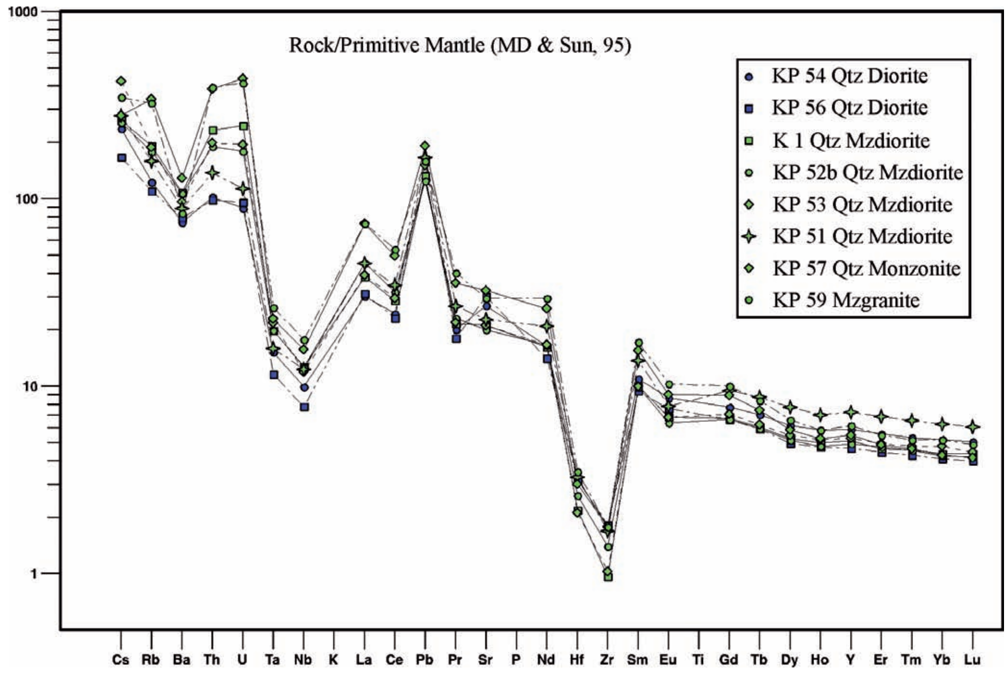

Fig. 8 - Incompatible trace element patterns for Kopaonik intrusive rocks. Element abundances are relative to Primitive Mantle (McDonough and Sun, 1995).

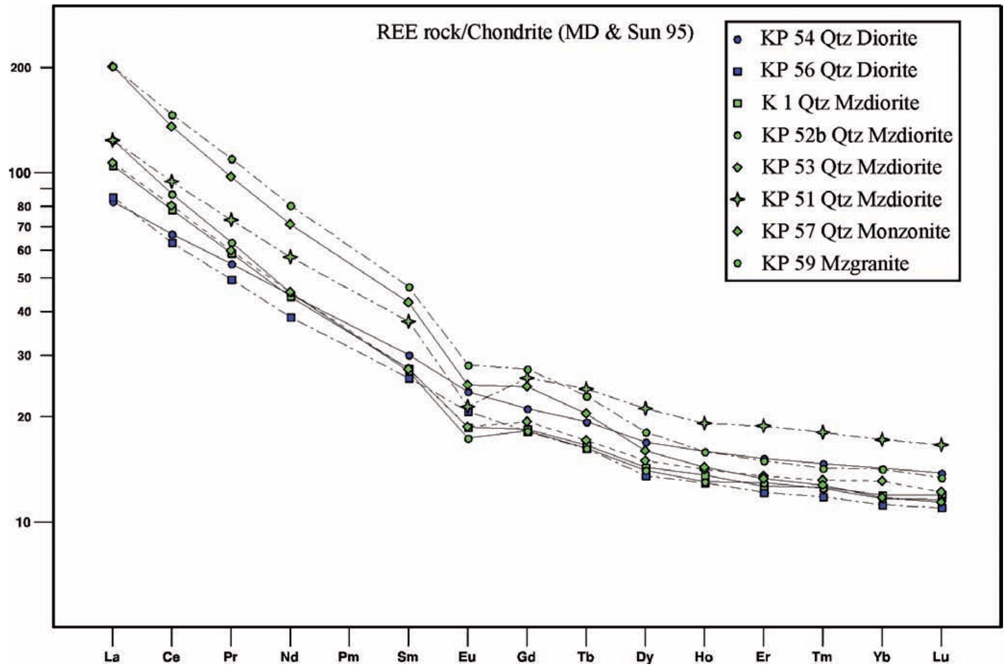

Fig. 9 - Rare Earth element patterns for Kopaonik intrusive rocks. Element abundances are relative to CI chondrites (McDonough and Sun, 1995).

plain the whole evolution pattern from dioritic rocks to qtz-monzonitic ones considering Nd isotopes, as well as the compatible elements, and the incompatible elements, except for Sr. This is particularly evident considering the Sr isotopes: in fact the dioritic rocks, which are less evolved and thus should be less contaminated do not have the lowest $^{87}Sr/^{86}Sr$ initial ratios and the lowest Sr contents. The AFC process is still a viable mechanism to explain evolution from quartz monzodiorites to quartz monzonites, but a dioritic end-member with lower Sr (≈ 400 ppm) and $^{87}Sr/^{86}Sr$ (≈ 0.7064) would be required to explain the observed variations through a single evolutionary trend (Fig. 11). Also mixing trajectories fit quite well the observed $^{143}Nd/^{144}Nd$ and trace element variation trends, with B facies generated by about 30-50% of basic end-member. Again, the model fails when applied to Sr abundance and Sr isotope

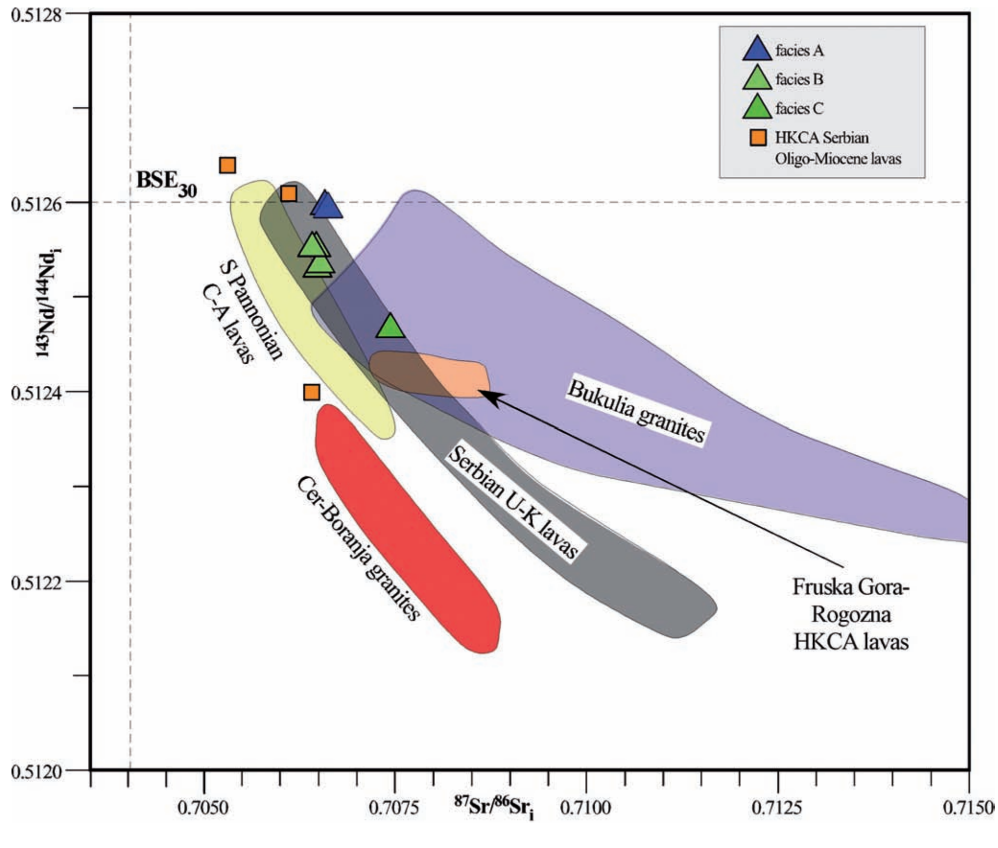

Fig. 10 - $^{143}Nd/^{144}Nd$ vs. $^{87}Sr/^{86}Sr$ isotope diagram for samples of Kopaonik intrusive complex and other Serbian magmatic rocks. Kopaonik data were corrected for t = 31.5 Ma, other data were corrected according their emplacement age. BSE_{30}, Bulk Silicate Earth corrected for t = 30 Ma. Literature data: South Pannonian Calc-Alkaline Lavas, Fruška Gora-Rogozna High-K Calc-Alkaline lavas and Cer-Boranja granitoids after Pamić and Balen (2001); High-K Calc-Alkaline Serbian Oligo-Miocene lavas and Serbian Utra-K lavas from Cvetković et al. (2004b); Bukulia granites, Cvetković et al. (2007b).

compositions, because the A facies diorites, which are the more primitive magmas of our dataset, having high MgO contents, high abundances of compatible elements, low abundances of incompatible elements, high $^{143}Nd/^{144}Nd$, may not represent the Sr- and ^{87}Sr-poor end member.

Thus, the dioritic rocks seem to be over-enriched in Sr, ^{87}Sr, and also CaO with respect to the evolutionary and/or mixing trends they depict according to their major, compatible and incompatible trace element contents, as well as Nd isotope ratios. We suggest that the Ca-Sr enrichment is a secondary feature of the dioritic rocks, acquired by magma-wallrock reactions during its final emplacement at shallow crustal level. This hypothesis is in agreement with geological evidence, which shows the dioritic facies to be the most external one of the Kopaonik Intrusive Complex, and the wallrock of the intrusive body to be made of meta-shales

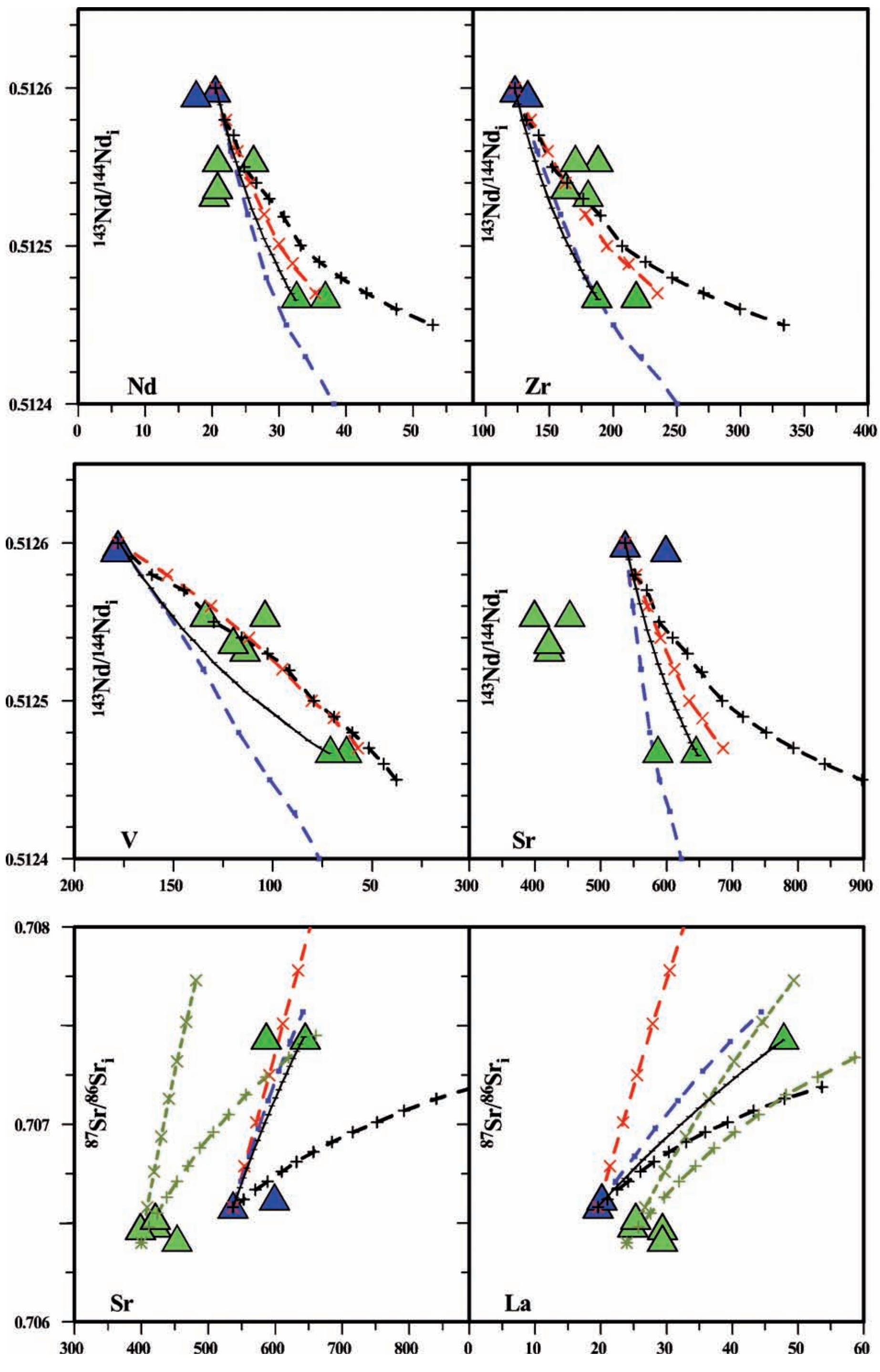

Fig. 11 - $^{143}Nd/^{144}Nd$ vs. V, Sr, Nd, Zr (ppm) and $^{87}Sr/^{86}Sr$ vs. Sr and La (ppm) plots for Kopaonik intrusive rocks. AFC trajectories (dashed lines) are drawn starting from sample KP 54, assuming a fractionation assemblage made up from of 40% amphibole, 40% plagioclase, 10% biotite, 7% quartz, 3% magnetite. Red curve, BK 134 as contaminant and R = 0.5 (R- assimilated mass/fractionated mass ratios). Blue curve, BK 136 as contaminant and R = 0.5. Black curve BK 136 as contaminant and R = 0.25. Green curves, BK 136 as contaminant, R = 0.3 and r = 0.5, respectively. Green curves start from a hypothetic end member with same composition of KP 54, except for Sr = 400 ppm, La = 24 ppm, $^{87}Sr/^{86}Sr = 0.7064$. Cross and dots represent 5% fractionation steps. Mixing trajectories (black solid line) drawn assuming KP 54 and KP 56 as end members.

and meta-carbonates. These latter rocks are part of a thermo-metamorphic aureole, characterized by both hornfels and skarn formation (e.g., Urošević et al., 1973a). Interaction between uprising magma and carbonatic rocks, which produced the skarn, may be also responsible for the Ca-Sr enrichment of the dioritic rocks.

In summary, the available data as well as the secondary Ca-Sr enrichment of the dioritic rocks do not allow to fully discriminate between AFC or mixing processes. However, the occurrence of cumulitic enclaves (Cvetković et al., 2002), and some evident linear correlations between major elements and modal abundances of mineral phases, such as MgO-Hbl, Al_2O_3-Pl (Fig. 7, insets), TiO_2-Bt and K_2O-Or, testify for the role played by crystal fractionation processes: thus, differentiation via AFC from a common magma is our preferred hypothesis to explain the petrographical, geochemical and isotopic variations in the studied rocks.

The collected data on the Kopaonik intrusives fall into the picture of regional Cenozoic magmatism proposed in some recent reviews (Pamić et al., 2002; Cvetković et al., 2007b; Kovacs et al., 2007), that suggest a continuous Late Paleogene-Middle Miocene magmatic belt developed throughout the Balkan Peninsula from the Eastern Alps to Northwestern Turkey. This magmatic belt includes plutonic and volcanic rocks, which vary both in evolutionary degree and in geochemical affinity, ranging from high-K calc-alkaline to shoshonitic to ultra-potassic. Anyway, all these products share geochemical and isotope evidence of a similar mantle source, enriched in LILE with respect to HFSE, in $^{87}Sr/^{86}Sr$ and depleted in $^{143}Nd/^{144}Nd$.

The most abundant and oldest products are high-K calc-alkaline, whereas the ultra-K products are scarce and generally younger; interestingly, these latter are not restricted to the Oligocene-Middle Miocene, but may be also significantly younger, as is the case of the Serbian and Macedonian latest Miocene to Pleistocene Lamproites (Cvetković et al., 2004a; Prelević et al., 2005; 2008, Yanev et al., 2008). This magmatic belt is usually genetically linked to subduction of the Neotethyan oceanic lithosphere under the Eurasia continental lithosphere. This eastward subduction started in the Early Jurassic, as deduced by the Middle Jurassic development of a wide supra-subduction oceanic basin and associated magmatic arc (Bortolotti et al., 2002; Brown and Robertson, 2004; Saccani et al., 2008a) and it was probably connected to the inception of subduction of continental lithosphere in the latest Jurassic (Bortolotti et al., 2005). Convergence affected also the supra-subduction oceanic basin, resulting in obduction and displacement of a large ophiolitic nappe onto the Adria continental margin. The obduction process was followed, probably in Early Cretaceous, by the collision that produced a wide suture zone where the pile of deformed oceanic and continental units was intruded by Late Jurassic calc-alkaline granitoids (Šarić et al., 2009). In this framework a strong modification of the mantle wedge by subduction-induced metasomatism was produced by dehydratation of the subducted oceanic slab. According to Cvetković et al. (2004b), this modified wedge, becoming more and more residual with time, can be regarded as the source of the magmatism, that, as recognized in the Kopaonik area, accompanied deformation during the Late Cretaceous-Eocene collisional and Oligocene-Miocene post-collisional phases. This interpretation agrees with the change in geochemical characteristics of the magmatic rocks during the time observed in the whole Dinaric-Hellenic Belt (Cvetković et al., 2004b and 2007b).

CONCLUSIONS

The intrusive complex cropping out in the Kopaonik area is characterized by a dome-like structure consisting of three concentric magmatic facies, with a gradual and continuous transition between them. The core of the Kopaonik Intrusive Complex is represented by coarse-grained porphyroid qtz-monzonites and minor monzogranites (facies C), surrounded by fine to medium grained granodiorites and qtz-monzodiorites (facies B). The external area of the intrusive body consists of fine-grained qtz-diorites (facies A), characterized by a well developed magmatic foliation. The boundaries with the host rocks, represented by the Kopaonik Metamorphic Complex, are marked by skarns and hornfels.

The collected data allow a more accurate characterization of this intrusive complex. First, the geochemical data indicate that Kopaonik granitoids are I-type, with high-K calc-alkaline affinity. The studied rocks are genetically and chemically linked to the coeval volcanic rocks that crop out in the area (Urošević et al., 1973a). A strong genetic relationship among the three facies is observed and the collected geological, petrographical and petrochemical data suggest that the different facies of the intrusive complex may be originated by crystal fractionation processes in a closed system. However, the observed Sr-Nd isotope ratios do not fit with this simple model and a more complex process, as mixing or, more probably, crystal fractionation combined with assimilation of crustal material, is here proposed, along with a shallow Ca-Sr enrichment of the external dioritic facies, probably due to contamination with the carbonate host rocks. Rb-Sr whole-rock-biotite age provides a minimum emplacement age of 31.5±0.3 Ma (Early Oligocene).

Finally, the data presented here allow to put the Kopaonik Intrusive Complex within the general framework of the Cenozoic magmatism of the Dinaric-Hellenic region proposed in the recent literature (e.g., Kovacs et al., 2007). The available data suggest a continuous Late Paleogene-Middle Miocene magmatic belt developed throughout the Balkan Peninsula from the Eastern Alps to Northwestern Turkey. This magmatic belt includes plutonic and volcanic rocks, which vary both in evolutionary degree and in geochemical affinity, from high-K calc-alkaline to shoshonitic to ultra-potassic. The origin of this magmatism is genetically linked with subduction of the Neotethyan oceanic lithosphere under the Eurasia continental lithosphere. In this picture, the source of the Kopaonik magmatic rocks can be identified in a mantle wedge strongly modified by subduction-induced metasomatism.

ACKNOWLEDGEMENTS

This research was supported by M.I.U.R. (Project PRIN, 2005 and 2006), by C.N.R (Istituto di Geoscienze e Georisorse) and by “Ateneo grants” funds of the Pisa University.

APPENDIX

Analytical methods

Petrographic and whole-rock major elements analyses were conducted on 12 samples of the Kopaonik Intrusive Complex. Major elements were determined by x-ray fluorescence on an ARL 9400 XP+ spectrometer; estimated precision (relative to standard deviation, RSD) is about 1% for SiO_2 and about 2% for the other major elements except for those with low concentrations (<0.50 wt.%), for which the absolute standard deviation is about ±0.01%. Loss on ignition (LOI) was determined by gravimetry at 1000 ºC after preheating at 110 ºC. The concentrations of a set of thirty-five trace elements were determined by inductively coupled plasma-mass spectrometry (VG PQII Plus) at the Dipartimento di Scienze della Terra, University of Pisa. Analytical precision, assessed by repeated analysis of the in-house standard HE-1 (Mt. Etna hawaiite), is between 2 and 5% RSD, except for Gd, Tm, Be, Sc, Pb (6-8% RSD). Rb, Sr, Zr and Y were determined via XRF too. Comparing XRF and ICP-MS data, it is evident that Zr determined via ICP-MS is markedly lower than the XRF one (about 1/10 ratio), due to the residual zircon undissolved by normal acid attack performed with standard ICP-MS analytical procedure. For this reason, Zr and Hf ICP-MS data will not be considered. Instead, Y XRF values are undistinguishable from Y ICP-MS values, if we consider the analytical errors; this means that negligible contents of Y and HREEs were partitioned into zircon, and that ICP-MS data for these elements can be considered valid.

Sr and Nd isotope compositions were measured with a Finnigan MAT 262 multi-collector mass spectrometer at the CNR Istituto di Geoscienze e Georisorse in Pisa. Conventional ion exchange methods were used for Sr and Nd separations. Measured $^{87}Sr/^{86}Sr$ ratios were normalized to $^{86}Sr/^{88}Sr = 0.1194$; $^{143}Nd/^{144}Nd$ ratios were normalized to $^{146}Nd/^{144}Nd = 0.7219$. During collection of the isotopic data for this study, replicate measurements of NIST SRM 987 ($SrCO_3$) and La Jolla standards yielded values of 0.710243±13 (2σ, N = 20) for $^{87}Sr/^{86}Sr$ and 0.511848±7 (2σ, N = 30) for $^{143}Nd/^{144}Nd$.

REFERENCES

Bortolotti V., Chiari M., Kodra A., Marcucci M., Marroni M., Pandolfi L., Prela M. Principi G. and Saccani E., 2007. Triassic MORB magmatism in the Southern Mirdita Zone (Albania). Ofioliti, 31 (1): 1-9.

Bortolotti V., Chiari M., Marcucci M., Marroni M., Pandolfi L., Principi G. and Saccani E. 2004. Comparison among the Albanian and Greek ophiolites, in search of constraints for the evolution of the Mesozoic Tethys ocean. Ofioliti, 29: 19-35.

Bortolotti V., Chiari M., Marcucci M., Photiades P., Principi G. and Saccani E., 2008. New geochemical and age data on the ophiolites from the Othrys area (Greece): implication for the Triassic evolution of the Vardar Ocean. Ofioliti, 33: 135-151

Bortolotti V., Marroni M., Pandolfi L. and Principi G., 2005. Mesozoic to Tertiary tectonic history of the Mirdita ophiolites, northern Albania. In: Y. Dilek, Y. Ogawa, V. Bortolotti and P. Spadea (Eds.), Evolution of ophiolites in convergent and divergent plate boundaries. Isl. Arc, 14: 471-493

Bortolotti V., Marroni M., Pandolfi L., Principi G. and Saccani E., 2002. Alternation of MOR and SSZ basalts in Albanian ophiolites: Evidences of interactions between Mid-Ocean Ridge and subduction-related processes in an infant arc setting. J. Geol., 110: 561-576.

Brown S.A.M. and Robertson A.H.F., 2004. Evidence for Neotethys rooted within the Vardar suture zone from Voras Massif, northernmost Greece. Tectonophysics, 381: 143-173.

Çollaku A., Cadet J. P., Bonneau M. and Jolivet L., 1992. L'édifice structural de l'Albanie septentrionale: des éléments de réponse sur les modalité de la mise en place des ophiolites. Bull. Soc. Géol. France, 163: 455-468.

Cvetković V., Downes H., Prelević D., Jovanović M. and Lazarov M., 2004a. Characteristics of the lithospheric mantle beneath east Serbia inferred from ultramafic xenoliths in Palaeogene basanites. Contrib. Mineral. Petrol., 148 (3): 335-357.

Cvetković V., Downesc H., Prelević D., Lazarov M. and Resimic-Šarić K., 2007a. Geodynamic significance of ultramafic xenoliths from Eastern Serbia: Relics of sub-arc oceanic mantle? J. Geodyn., 43: 504-527.

Cvetković V., Harkovska A., Karamata S., Knežević V., Memović E. and Pécskay Z., 1995. Correlation of some Oligocene volcanic complexes along the W - E traverse in Central Balkan Peninsula. 15th CBGA Congr., Sofia, Abs., p. 1186-1189.

Cvetković V., Poli G., Christofides G., Koroneos A., Pécskay Z., Resimic-Šarić, K. and Eric V., 2007b. The Miocene granitoid rocks of Mt. Bukulja (central Serbia): evidence for Pannonian extension-related granitoid magmatism in the northern Dinarides. Eur. J. Mineral., 19: 513-532.

Cvetković V., Poli G., Resimić-Šarić K. Prelević D. and Lazarov M., 2002. Tertiary post-collision granitoid of Mt. Kopaonik (Serbia) - Petrogenetic constraints based on new geochemical data. Proceed. 17th Congr. Carpathian-Balkan Geol. Ass., Bratislava, September 2002.

Cvetković V., Prelević D., Downes H., Jovanović M., Vaselli O. and Pécskay Z., 2004b. Origin and geodynamic significance of Tertiary postcollisional basaltic magmatism in Serbia (central Balkan Peninsula). Lithos, 73 (3-4): 161-186,

Cvetković V., Prelević D. and Pécskay Z. 2000. Lamprophyric rocks of the Miocene Borac eruptive complex (Central Serbia, Yugoslavia). Acta Geol. Hung., 43 (1): 25-41.

De Paolo D.J., 1981. Trace element and isotopic effects of combined wall rock assimilation and fractional crystallization. Earth Planet. Sci. Lett., 53: 189-202.

Dimitrijević M.D., 1997. Geology of Jugoslavia. Beograd, Geoinstitut-Barex, 187 pp.

Dimitrijević M.D., 2001. Dinarides and Vardar Zone: a short review of the geology. Acta Vulcan., 13: 1-8.

Dilek Y., Shallo M. and Furnes H., 2005. Rift-drift, seafloor spreading, and subduction tectonics of Albanian ophiolites. Intern. Geol. Rev., 47: 147-176

Djordjević M., 2005. Volcanogenic Turonian and epiclastics of Senonian in the Timok Magmatic Complex between Bor and the Tupiznica Mountain (eastern Serbia). Ann. Géol. Pénins. Balkan., 66: 63-71.

Gaggero L., Marroni M., Pandolfi L. and Buzzi L., 2009. Modelling of oceanic lithosphere obduction: constraints from the metamorphic sole of Mirdita ophiolites (Northern Albania). Ofioliti, 34: 17-43.

Karamata S., 1994. The evolution of the northern part of the Vardar Zone in Mesozoic. Bull. Geol. Soc. Greece, 30 (2); 479-486.

Karamata S., 2006. The geodynamical framework of the Balkan Peninsula: its origin due to the approach, collision and compression of Gondwana and Eurasian units. In: A.H.F. Robertson and D. Mountrakis (Eds.), Tectonic development of the Eastern Mediterranean Region. Geol. Soc. London Spec. Publ., 260: 155-178.

Karamata S., Delaloye M., Lovrić A. and Knežević V., 1992a. Two genetic groups of Tertiary granitic rocks of central and western Serbia. Geol. Ann. Balk. Poluos., Belgrade, 56: 263-283.

Karamata S., Olujić J., Protic L., Milovanović D., Vujnović L., Popević A., Memović E., Radovanović Z. and Resimić-Šarić K., 2000. The western belt of the Vardar Zone - the remnant of a marginal sea. In: S. Karamata and S. Jankovic (Eds.), Geology and metallogeny of the Dinarides and the Vardar Zone. Acad. Sci. Arts Republic Serbia, Collections and Monographs 1, pp.

Karamata S., Stojanov R., Serafimovski T., Boev B. and Aleksandrov M., 1992b. Tertiary magmatism of the Vardar Zone of the Dinarides and Serbo-Macedonian Mass. Geol. Macedon., 6: 127-186.

Kilias A., Falalakis G. and Mountrakis D., 1999. Cretaceous-Tertiary structures and kinematics of the Serbomacedonian metamorphic rocks and their relation to the exhumation of the Hellenic hinterland (Macedonia, Greece). Interm. J. Earth Sci., 88: 513-531.

Knežević V., Karamata S. and Cvetković V., 1994. Tertiary granitic rocks along the southern margin of the Pannonian Basin. Mineral. Petrog. Acta, 35: 71-80.

Kovács I., Csontos L., Szabó Cs., Bali E., Falus Gy., Benedek K. and Zajacz Z., 2007 Paleogene-Early Miocene igneous rocks and geodynamic of the Alpine-Carpathian-Pannonian-Dinaric region: An integrated approach. Geol. Soc. Am. Spec. Paper, 418: 93-112.

Ludwig K., 2003. K. Isoplot/Ex version 2.05. A geochronological toolkit for Microsoft Excel, Berkeley Geochron. Center.

Marroni M., Pandolfi L., Saccani E. and Zelić M., 2004. Boninites from the Kopaonik area (southern Serbia): evidences for supra-subduction ophiolites in the Vardar Zone. Ofioliti 29: 251-254.

McDonough W.F. and Sun S.S., 1995. The composition of the Earth. Chem. Geol., 120: 223-253.

Milovanović D., Marchig V. and Karamata S., 1995. Petrology of the crossite schist from Fruška Gora Mts. (Yugoslavia), relic of a subducted slab of the tethyan oceanic crust. J. Geodyn., 20 (3): 289-304

Pamić J., 1993. Eoalpine to Neoalpine magmatic and metamorphic processes in the northwestern Vardar Zone, the easternmost Periadriatic Zone and the southwestern Pannonian Basin. The origin of sedimentary basins; inferences from quantitative modelling and basin analysis. Tectonophysics, 226: 503-518.

Pamić J., 1997. Volcanic rocks of the Sava-Drava interfluve and Baranja. Nafta Monograph, Zagreb, 192 pp.

Pamić J. and Balen D., 2001. Tertiary magmatism of the Dinarides and the adjoining South Pannonian Basin. Acta Vulcan., 13: 9-24.

Pamić J., Gusić I. and Jelaska V., 1998. Geodynamic evolution of the central Dinarides. Tectonophysics, 297: 251-268.

Pamić J. and Lanphere M.A., 1991. Alpine A-type granites from the collisional area of the northernmost Dinarides and Pannonian Basin. N. Jb. Mineral. Abh., 162: 215-236.

Pamić J., Pécskay Z. and Balen D., 2000. Lower Oligocene K-Ar ages of high-K calc-alkaline and shoshonite rocks from the north Dinarides in Bosnia. Mineral. Petrol., 70 (3/4): 313-320.

Pamić J., Tomljienovic B. and Balen D., 2002. Geodynamic and petrogenesis evolution of Alpine ophiolites from the central and NW Dinarides; an overview. Lithos, 65: 113-142.

Peccerillo A. and Taylor S.R., 1976. Geochemistry of Eocene calc-alkaline volcanic rocks from the Kastamonu area, northern Turkey. Contrib. Mineral. Petrol., 58: 63-81.

Prelević D., Foley S.F., Romer R. and Conticelli S., 2008. Mediterranean Tertiary lamproites derived from multiple source components in postcollisional geodynamics. Geochim. Cosmochim. Acta, 72: 2125-2156.

Prelević D., Foley S.F., Romer R. L., Cvetković V. and Downes H., 2005. Tertiary ultrapotassic volcanism in serbia: constraints on petrogenesis and mantle source characteristics. J. Petrol., 46: 1443-1487

Robertson A.H.F. and Karamata S., 1994. The role of subduction-accretion processes in the tectonic evolution of the mesozoic tethys in Serbia. Tectonophysics, 234: 73-94.

Robertson A.H.F., Karamata S. and Šarić K., 2009. Overview of ophiolites and related units in the Late Palaeozoic-Early Cenozoic magmatic and tectonic development of Tethys in the northern part of the Balkan region. Lithos, 108: 1-36.

Saccani E., Beccaluva L., Coltorti M. and Siena F., 2004. Petrogenesis and tectono-magmatic significance of the Albanide - Hellenide Subpelagonian ophiolites. Ofioliti, 29: 75-93.

Saccani E., Bortolotti V., Marroni M., Pandolfi L. and Photiades A., 2008b. The Jurassic association of backarc basin ophiolites and calc-alkaline volcanics in the Guevgueli Complex (Northern Greece): implication for the evolution of the Vardar Zone. Ofioliti, 33: 209-227

Saccani E., Photiades A., Santato A. and Zeda O., 2008a. New evidence for supra-subduction zone ophiolites in the Vardar Zone of Northern Greece: implications for the tectono-magmatic evolution of the Vardar oceanic basin. Ofioliti, 33: 65-85

Šarić K., Cvetković V., Romer R.L., Christofides G. and Koroneos A., 2009. Granitoids associated with East Vardar ophiolites (Serbia, F.Y.R. of Macedonia and northern Greece): Origin, evolution and geodynamic significance inferred from major and trace element data and Sr-Nd-Pb isotopes. Lithos, 108: 131-150

Schmid S.M., Bernoulli D., Fügenschuh B., Matenco L., Schefer S., Schuster R., Tischler M. and Ustaszewski K., 2008. The Alpine-Carpathian-Dinaridic orogenic system: correlation and evolution of tectonic units. Swiss J. Geosci., 101: 139-183.

Sudar M., 1986. Mikrofosili i biostratigrafija trijasa unutrashnjikh Dinarida Jugoslavije izmedju Gucheva i Ljubishnje. Geol. Anali Balkan. Poluostrva, 50: 151-394.

Taylor S.R. and McLennan S.M., 1985. The continental crust: its composition and evolution, Oxford (UK), Blackwell, 312 pp.

Urošević M., Pavlović Z., Klisić M., Brković T., Malešević M., Trifunović S., Stafanović M. and Marković O., 1973a. Geological map and explanatory notes of the sheet “Vrnjci”. Savezni Geol. Zavod, Beograd, 69 pp.

Urošević M., Pavlović Z., Klisić M., Brković T., Malešević M., Trifunović S., Karamata S. and Stefanović M., 1973b. Geological map and explanatory text of the sheet Novi Pazar. Savezni Geol. Zavod, Beograd, p. 1-77.

Yanev Y., Boev B., Doglioni C., Innocenti F., Manetti P., Pecskay Z., Tonarini S. and D’Orazio M., 2008. Late Miocene to Pleistocene potassic volcanism in the Republic of Macedonia . Mineral. Petrol., 94: 45-60.

Zelic M., D’Orazio M., Malasoma A., Marroni M. and Pandolfi L., 2005. The metabasites from the Kopaonik metamorphic complex, Vardar Zone, southern Serbia: remnants of the rifting-related magmatism of the Mesothetyan domain or evidence for Paleotethys closure in the Dinaric-Hellenic belt? Ofioliti, 30: 91-101.

Zelic M., Levi N., Malasoma A., Marroni M., Pandolfi L. and Trivić B., 2010. Alpine tectono-metamorphic history of the continental units from Vardar Zone: the example of Kopaonik metamorphic complex (Dinaric-Hellenic Belt, Serbia). Geol. J., in press. DOI: 10.1002/gj.1169.

Received, July 17, 2009
Accepted, April 15, 2010